



Detection of Severity of Bearing Cage fault of Induction Motor with Externally Induced Vibration

Abhishek Gupta¹, Rohank Agarwal², Manan Temani³, Rahul Kr. Gangwar⁴

B.Tech Student, Dept. of EE, Indian School of Mines, Dhanbad, Jharkhand, India^{1 2 4}

B.Tech Student, Dept. of ECE, Indian School of Mines, Dhanbad, Jharkhand, India³

ABSTRACT: Induction machines play a vital role in industry and there is a strong demand for their reliable and safe operation. Failure of its performance leads to shut down and loss of revenue as well as time. Bearing Fault accounts to maximum percentage among all faults pertaining to Induction machines. This paper presents approach to determine severity of cage fault in bearing with the help of dynamic model based on contact mechanics applied to case of external harmonic excitation. The paper focuses on air gap variation to predict fault frequencies and loss of stiffness in rolling element bearings.

KEYWORDS: Induction motor, condition monitoring, Bearing fault, airgaps.

I. INTRODUCTION

Induction Motors are the most widely used electrical machine mainly because of its simple structure, high reliability and ruggedness. In an industrialized nation, they can consume between 40 to 50 % of total generated capacity of that country [1]. However, owing to the thermal, electrical and mechanical stresses, mechanical and electrical failures are unavoidable in induction motors. Early detection of abnormalities in the motor will help to avoid expensive failures.

Failure statistics have reported that percentage failure by components in induction motor is typically:

- Stator fault (38%)
- Rotor fault (10%)
- Bearing fault (40%)
- Other fault (12%)

Many papers can be found in the literature concerning the general condition monitoring of induction machines [2, 3, 4]. The distribution of failures within the machine subassemblies is reported in many reliability survey papers [5], [6].

Bearings are common elements in electrical machine employed to permit rotary motion of the shafts. Rolling bearings are used in almost every industrial process involving rotating and reciprocating machinery [7]. Bearing consists of two rings called inner and outer rings and a set of balls or rolling elements rotating inside these rings. A continued stress on the bearing causes fatigue failures, usually at the inner or outer races of the bearings. Rolling elements are bounded by a cage which assures equidistance between the balls. Localized faults will produce characteristic vibration frequency components. The different faults that occur in bearing are outer raceway fault, inner raceway fault, ball fault and cage fault. Since ball bearing support the rotors, any bearing defect will produce a radial motion between the rotor and stator of the machine. The mechanical displacement resulting from damaged bearing causes the machine air gap to vary in a manner that can be described by a combination of rotating eccentricities moving in both directions.

In industrial applications, bearings are critical mechanical components. Proper functioning of the equipment depends, to a great extent, on the smooth running of the bearings. Bearing faults that are not detected in time cause malfunction, loss of performance, and reduced efficiency [8], [9] and may even lead to catastrophic failure of the machinery. Vibration signals are usually employed to detect the presence of mechanical faults in bearings. In many situations, diagnostic methods based on the analysis of the vibration signals have proved their effectiveness [10], [11]. Analysis of

International Journal of Advanced Research in Electrical, Electronics and Instrumentation Engineering

(An ISO 3297: 2007 Certified Organization)

Vol. 3, Issue 4, April 2014

vibration spectra can be used to determine characteristic fault frequency for the particular bearing fault. The paper focusses on cage fault detection and its severity estimation supported by simulation results and graphs.

II. RELATED WORK

Among the mechanical problems detected by vibration spectra, there are imbalance, misalignment, loose fitting, bent shaft, and bearing localized faults. Simplified kinematic models of the mechanical components (rolling bearings and meshing gears) are usually employed to simulate fault response of the machine drive train, in order to predict fault frequencies [12], [13]. The relationship between vibration and current in induction motors operated under external vibrations is investigated in [14]. It presents bearing fault model for induction motor based on contact mechanics under cage fault, together with experimental characterization of the machine rotor and results obtained from external shaker excitation experiment. It has dealt with the fault diagnosis of roller bearings applied to an induction machine operated under external vibration, employing vibration analysis and MCSA according to the airgap variation model. In this paper we propose an approach to detect severity of bearing cage fault based on model presented in [14].

III. BEARING FAULT MODEL WITH HARMONIC EXCITATION

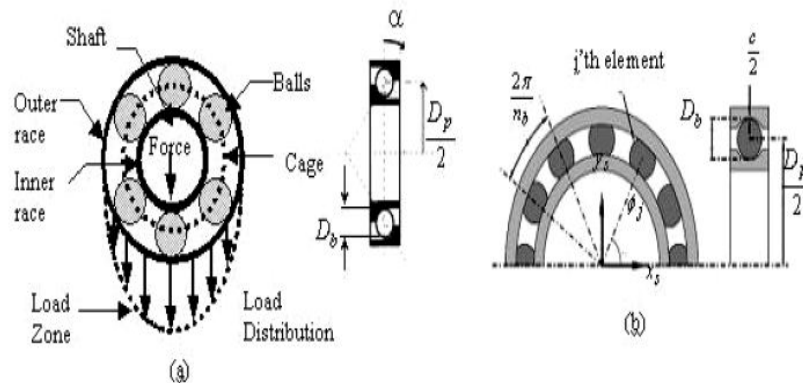


Figure 1. Bearing elements and its parameters

Figure 1(a) illustrates the main components of the rolling element bearing model and shows the load zone associated with the distribution of radial loads in the REB (Rolling element bearing) as it supports the shaft. Figure- 1(b) explains the essentials of the bearing model.

Radial bearings consist of two concentric rings or races, outer and inner, separated by balls or rollers (Fig. 1(a)). Rolling elements are bound by a cage: a component that maintains a constant angular pitch between adjacent rolling elements and prevents any contact. Localized faults will produce characteristic vibration frequency components. These bearing fault frequencies are a function of the bearing geometry, the operating speed, and whether the outer or the inner ring is fixed to the frame.

$$F_{cage} = \frac{1}{2} F_r \left(1 - \frac{D_b \cos \alpha}{D_p} \right) \quad (1)$$

F_r = Rotor mechanical frequency

F_{cage} = Cage fault frequency

D_b = Diameter of rolling spheres

D_p = Pitch diameter

α = Contact angle

International Journal of Advanced Research in Electrical, Electronics and Instrumentation Engineering

(An ISO 3297: 2007 Certified Organization)

Vol. 3, Issue 4, April 2014

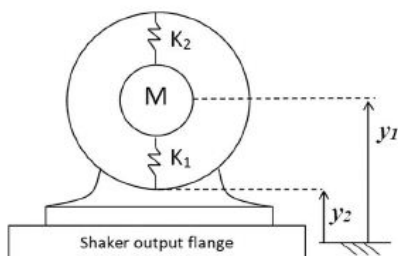


Figure 2. Equivalent model of rotor supported by harmonic exciter

In order to keep the model simple, only three force components will be considered:

- 1) The force supplied by the shaker;
- 2) The weight of the rotor and shaft;
- 3) The variable stiffness distribution of the bearing.

In particular, the rotor is represented by a suspended mass M (comprising rotor, shaft, and inner races) connected with the stator by means of a spring K_1 and K_2 . Nominally, K_1 and K_2 are equal for a healthy bearing; they differ from each other when a fault is present (e.g., rolling element removal) as shown in Figure 2.

The shaker provides a harmonic excitation, represented by

$$y_2(t) = A_{shaker} \cos(2\pi f_{shaker} t + \Phi_{shaker}) \quad (2)$$

where A_{shaker} , f_{shaker} and Φ_{shaker} are amplitude, frequency, and phase of the excitation displacement respectively given that y_1 and y_2 are displacement of rotor and harmonic shaker respectively.

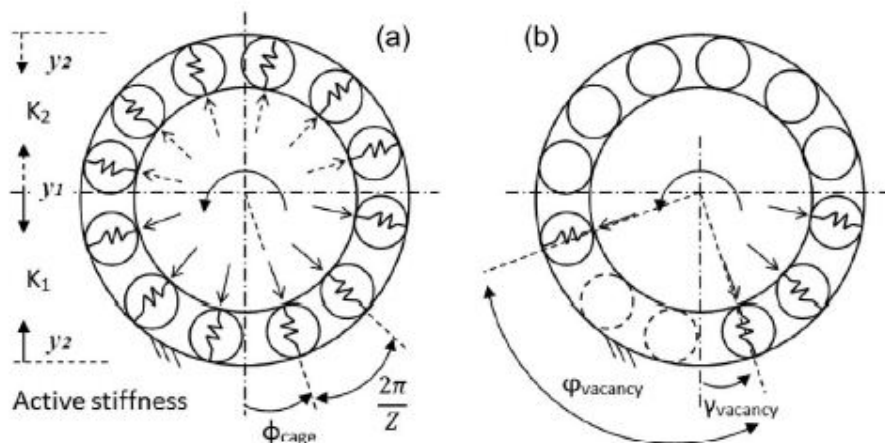


Figure 3. Load distribution among spheres in (a) healthy bearing (b) Faulty Bearing (two spheres removed)

Furthermore, taking into account the geometric distribution, stiffness is not only dependent upon the number of spheres present but also on their relative positions. Fig. 3(a) shows how each sphere contributes to the equivalent stiffness of the bearing. The equivalent stiffness is the sum of each contribution (as the modeled springs are in parallel configuration), while the single contribution depends on the angle Φ_{cage} between the angular position of the sphere and the reference axis. Contact mechanics theory is then applied to the system. According to Hertz's contact theory, the sphere radial deformation is proportional to the contact force raised to the $2/3$ power. The force contribution of each sphere along the load direction can be expressed as:



International Journal of Advanced Research in Electrical, Electronics and Instrumentation Engineering

(An ISO 3297: 2007 Certified Organization)

Vol. 3, Issue 4, April 2014

$$Q = \sum_i^Z P_i \cos \left(\Phi_{cage} + i \frac{2\pi}{Z} \right) \quad (3)$$

Where P_i is the force exerted by the generic i^{th} sphere. It must be noticed that, in a healthy bearing, the sphere configuration repeats with a $2\pi/Z$ period (where Z is the number of spheres).

Equivalent stiffness is thus given by:

$$K_{eq} = k_{sphere} \sum_i^Z \delta_{lj} \cos^{5/2} \left(\Phi_{cage} + i \frac{2\pi}{Z} \right) \quad (4)$$

where k_{sphere} is assumed to be equal to Young's module of steel. The δ_{lj} is the Kronecker delta, with l and j being its conditions, expressed as

$$l = \text{sign} \left[\cos \left(\Phi_{cage} + i \frac{2\pi}{Z} \right) \right] \quad (5)$$

$$j = \text{sign}(\Delta y_0 + y_2 - y_1) \quad (6)$$

where the function $\text{sign}[x]$ returns +1 if the argument is positive, -1 if the argument is negative, and 0 if otherwise and Δy_0 is the distance ($y_1 - y_2$) in the reference condition (motor and shaker stopped). With reference to Fig. 3(a), (4) can be easily explained: When the shaft is moving downward with respect to the reference condition, only the spheres below the horizontal line of symmetry are loaded. In this case, the sign of (6) is positive, and only the spheres lying in the bottom part (force components with solid line) give a contribution to the equivalent stiffness since the sign of (5) is positive in this region. On the other hand, when the shaft is moving upward with respect to the neutral position, (6) is negative, and only the spheres lying in the upper part (force components with dotted line) give a negative output to (5); then, they are counted in the computation of the respective equivalent stiffness. Hence, the equivalent stiffness became equal to $K1$ when the shaft is moving downward, while it is equal to $K2$ when it is moving upward.

A. CREATION OF FAULT IN BEARING OF INDUCTION MOTOR

When N spheres are removed from the bearing, the unsupported vacancy zone can be modeled as a superimposition of a cyclic phenomenon with the same rotating frequency of the cage. Fig. 3(b) shows an example with two spheres removed.

An initial phase $\gamma_{vacancy}$ of the vacancy location with reference to the vertical axis may be chosen but is assumed to be zero in the simulation without loss of generality. The equivalent stiffness of the faulty bearing can now be obtained as

$$K_{eq} = k_{sphere} \sum_i^Z \delta_{lj} v_i \cos^{5/2} \left(\Phi_{cage} + i \frac{2\pi}{Z} \right) \quad (7)$$

where

$$v_i = \left(i \frac{2\pi}{Z} \right) \notin [\gamma_{vacancy}; N \frac{2\pi}{Z} + \gamma_{vacancy}] \quad (8)$$

Equation (8) returns 0 if the term $i2\pi/Z$ belongs to the given interval and 1 if otherwise.

The equation of the system dynamics can then be expressed as

$$M\ddot{y}_1 + c(\dot{y}_1 - \dot{y}_2) + K_{eq}(y_1 - y_2) = F_{weight} \quad (9)$$

where, as mentioned before, M is mass of rotor, K_{eq} the equivalent stiffness coefficient and F_{weight} the weight of combined mass of rotor and shaft and the viscous damping coefficient c is assumed proportional to a fraction of the equivalent stiffness for stabilization purposes only.

IV. SIMULATION AND RESULTS

From a mechanical point of view, the loss of spheres translates in an increased clearance between the contacting bearing components. This causes a reduction of the stiffness and increases the mobility of the shaft in the radial direction. This usually leads to the appearance of a peak at F_{cage} in the vibration spectrum. If the external radial load is a harmonic motion (e.g., shaker vibration) which is our case of interest, it acts on the bearing with a push-pull excitation, and the unsupported area is aligned to the force direction twice per revolution. Hence, the effect of the varying stiffness in case of cage fault is seen as dominant peak at $2F_{cage}$ in the vibration spectrum.

International Journal of Advanced Research in Electrical, Electronics and Instrumentation Engineering

(An ISO 3297: 2007 Certified Organization)

Vol. 3, Issue 4, April 2014

The viscous damping coefficient c is assumed proportional to the equivalent stiffness (0.1%), and the stiffness of a single sphere K_{sphere} is set equal to Young's module of steel (210 000 N/mm²). Magnitude of shaker's amplitude is assumed to be equal to 2 units while its frequency is set equal to 1100 Hz. Frequency of cage is calculated by equation (1) and is found to be equal to 11.9 Hz. Total number of balls inside bearing is set equal to 24 and in order to calculate severity of fault due to vacancy or dislocation of balls value of n is varied in given Matlab model. Fig. 4 shows the block diagram of the Matlab model.

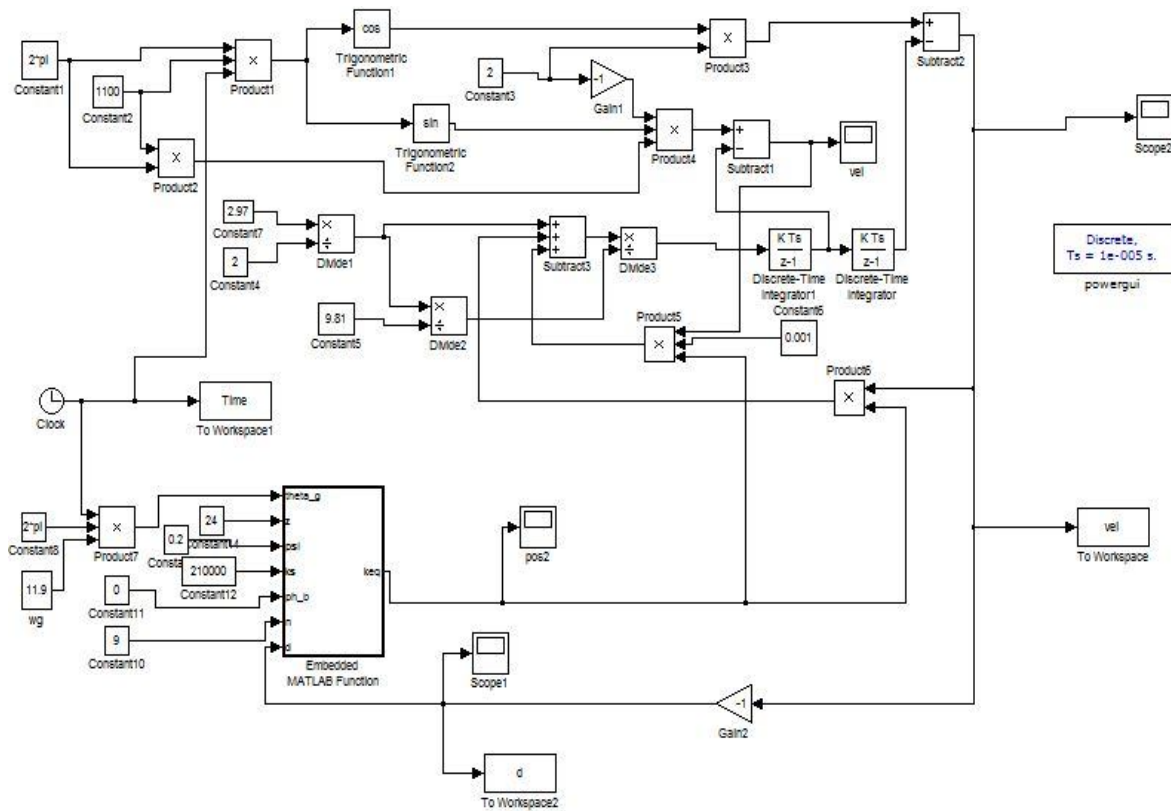


Figure 4. Simulink model of the bearing system with cage fault.

In order to calculate severity of fault, number of vacant spheres are increased varying from healthy bearing (no balls removed) to 6 balls removed from bearing and it is found that amplitude of second harmonic component i.e. at $2F_{cage}$ (23.8 Hz) keep on increasing with increased vacancy in bearing but for a healthy bearing with no balls removed it is found that there is no second harmonic component which is expected as plotted in fig. 5(b). The radial vibration of the rotor with respect to the stator was computed, and the resulting waveform is plotted in Fig. 5(a), 6(a),7(a) and 8(a). Demodulation of this radial vibration signal reveals a dominant component that is equal to the second harmonic of the rotational frequency of the cage for faulty bearing as expected from the discussion above (Fig. 6(b), 7(b) and 8(b)).Results of four cases taken are tabulated as:

International Journal of Advanced Research in Electrical, Electronics and Instrumentation Engineering

(An ISO 3297: 2007 Certified Organization)

Vol. 3, Issue 4, April 2014

TABLE 1. HARMONIC COMPONENT AND ITS AMPLITUDE

NUMBER OF BALLS REMOVED	DOMINANT HARMONIC COMPONENT	AMPLITUDE OF RESULTING HARMONIC
No balls removed	No second harmonic component	No second harmonic amplitude
Two balls removed	23.8 Hz= $2F_{cage}$	0.03896 unit
Four balls removed	23.8 Hz= $2F_{cage}$	0.08099 unit
Six balls removed	23.8 Hz= $2F_{cage}$	0.1031 unit

From TABLE 1. it is clearly found that amplitude of second harmonic component increases with the number of balls removed in the simulation model.

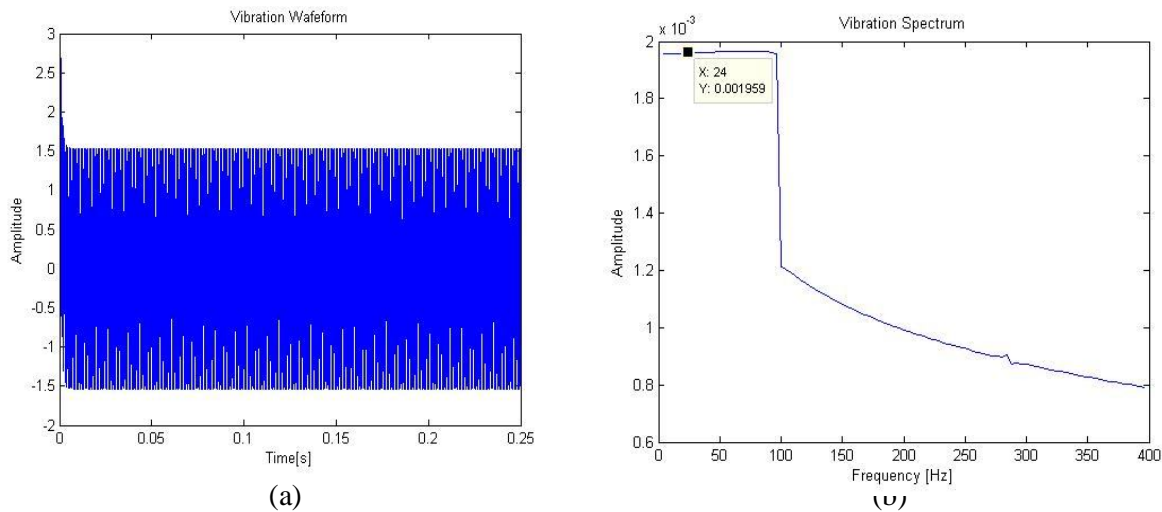


Figure 5. Radial vibration and vibration spectrum of shaft of healthy bearing (no balls removed)

Figure 5. Shows the radial vibration waveform and spectrum in case of healthy bearing (no balls removed). It is found that there is no dominant second harmonic peak which is characteristic of cage fault which is same as expected theoretically. Hence no cage fault is present in this case.

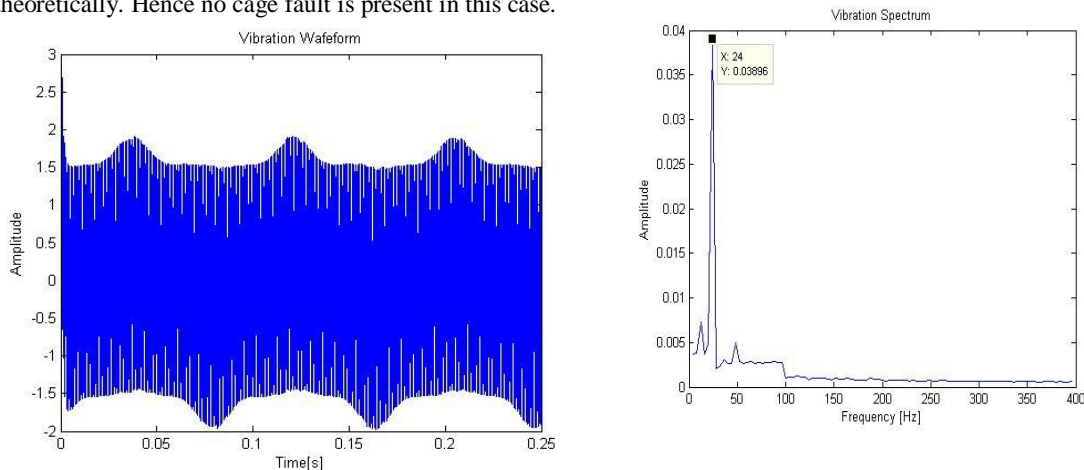


Figure 6:(a) Radial vibration waveform and (b) vibration spectrum of shaft of faulty bearing (two balls removed)

International Journal of Advanced Research in Electrical, Electronics and Instrumentation Engineering

(An ISO 3297: 2007 Certified Organization)

Vol. 3, Issue 4, April 2014

Figure 6. shows the plots in case of faulty bearing having cage fault with two balls removed in the simulation model parameter. The resulting vibration spectrum is found to have peaks at F_{cage} , $2F_{cage}$, $3F_{cage}$ and $4F_{cage}$. However the dominant peak occurs at $2F_{cage}$ with a magnitude of 0.03896 unit as marked in the figure.

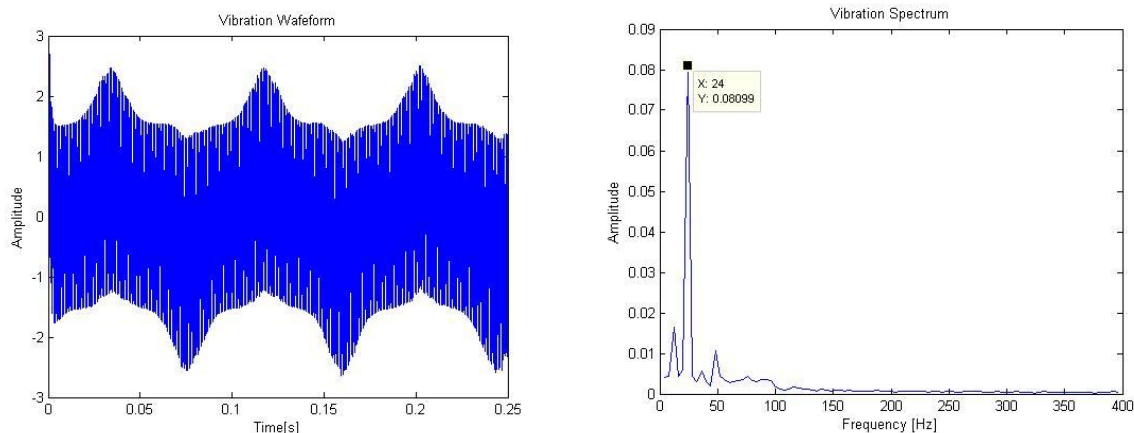


Figure 7:(a) Radial vibration Waveform and (b) vibration spectrum of shaft of faulty bearing(four balls removed)

In Figure 7(b) and 8(b) the dominant peak occurs at $2F_{cage}$ but with magnitude of 0.08099 unit(four balls removed) and 0.1031 unit(six balls removed) respectively. This increase in magnitude of harmonic component with increase in vacancy is deterministic of the cage fault severity.

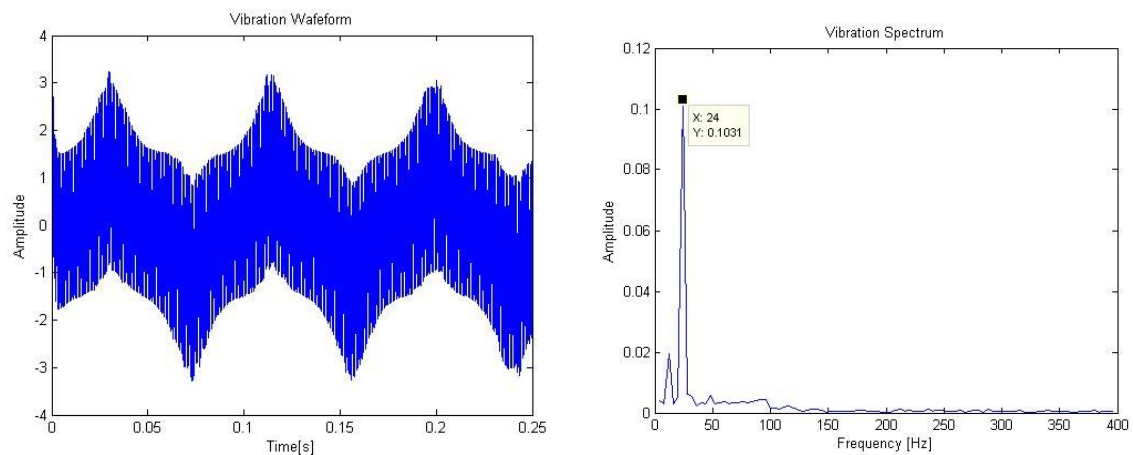


Figure 8:(a)Radial vibration waveform and (b) vibration spectrum of shaft of faulty bearing(six balls removed)



International Journal of Advanced Research in Electrical, Electronics and Instrumentation Engineering

(An ISO 3297: 2007 Certified Organization)

Vol. 3, Issue 4, April 2014

V.CONCLUSION

Kinematic Bearing model based on contact mechanics was simulated under external harmonic excitation. On analysis of the vibration spectrum a dominant harmonic is found at $2F_{\text{cage}}$ whose magnitude changes with the severity of cage fault due to loss of stiffness depending upon number of balls removed in the simulation model. Thus the severity of cage fault can be determined from vibration spectrum up to certain number of balls.

REFERENCES

- [1] Arfat siddique, G. S. Yadava, and Bhim singh, "a review of stator fault monitoring techniques of induction motors", Ieee transactions on energy conversion, vol. 20, no.1, march 2005.
- [2] S. Nandi, H. A. Toliyat, and X. Li, "Condition monitoring and fault diagnosis of electrical motors—A review," *IEEE Trans. Energy Convers.*, vol. 20, no. 4, pp. 719–729, Dec. 2005.
- [3] A. Bellini, F. Filippetti, C. Tassoni, and G. A. Capolino, "Advances in diagnostic techniques for induction machines," *IEEE Trans. Ind. Electron.*, vol. 55, no. 12, pp. 4109–4126, Dec. 2008.
- [4] A. Garcia-Perez, R. de Jesus Romero-Troncoso, E. Cabal-Yepez, and R. Osornio-Rios, "The application of high-resolution spectral analysis for identifying multiple combined faults in induction motors," *IEEE Trans. Ind. Electron.*, vol. 58, no. 5, pp. 2002–2010, May 2011.
- [5] O. V. Thorsen and M. Dalva, "A survey of faults on induction motors in offshore oil industry, petrochemical industry, gas terminals, and oil refineries," *IEEE Trans. Ind. Appl.*, vol. 31, no. 5, pp. 1186–1196, Sep./Oct. 1995.
- [6] A. H. Bonnett, "Root cause AC motor failure analysis with a focus on shaft failures," *IEEE Trans. Ind. Appl.*, vol. 36, no. 5, pp. 1435–1448, Sep./Oct. 2000
- [7] C. Bianchini, F. Immovilli, M. Cocconcelli, R. Rubini, and A. Bellini, "Fault detection of linear bearings in brushless ac linear motors by vibration analysis," *IEEE Trans. Ind. Electron.*, vol. 58, no. 5, pp. 1684–1694, May 2011.
- [8] G. Curcuru', M. Cocconcelli, F. Immovilli, and R. Rubini, "On the detection of distributed roughness on ball bearings via stator current energy: Experimental results," *Diagnostyka*, vol. 51, no. 3, pp. 17–21, 2009.
- [9] L. Frosini and E. Bassi, "Stator current and motor efficiency as indicators for different types of bearing faults in induction motors," *IEEE Trans. Ind. Electron.*, vol. 57, no. 1, pp. 244–251, Jan. 2010.
- [10] R. Rubini and U. Meneghetti, "Application of the envelope and wavelet transform analysis for the diagnosis of incipient faults in ball bearings," *Mech. Syst. Signal. Process.*, vol. 15, no. 2, pp. 287–302, Mar. 2001.
- [11] J. R. Stack, T. G. Habetler, and R. G. Harley, "Fault-signature modeling and detection of inner-race bearing faults," *IEEE Trans. Ind. Appl.*, vol. 42, no. 1, pp. 61–68, Jan./Feb. 2006.
- [12] N. Sawalhi and R. Randall, "Simulating gear and bearing interactions in the presence of faults: Part I. The combined gear bearing dynamic model and the simulation of localised bearing faults," *Mech. Syst. Signal Process.*, vol. 22, no. 8, pp. 1924–1951, Nov. 2008.
- [13] N. Sawalhi and R. Randall, "Simulating gear and bearing interactions in the presence of faults: Part II: Simulation of the vibrations produced by extended bearing faults," *Mech. Syst. Signal Process.*, vol. 22, no. 8, pp. 1924–1951, Nov. 2008.
- [14] Immovilli, F., Bianchini, C., Cocconcelli, M., Bellini, A., & Rubini, R. (2013). Bearing fault model for induction motor with externally induced vibration. *Industrial Electronics, IEEE Transactions on*, 60(8), 3408-3418.
- [15] Mehala, Neelam. "Condition monitoring and fault diagnosis of induction motor using motor current signature analysis." *Unpublished doctoral dissertation, National Institute of Technology Kurukshetra, India* (2010).